

## Supplementary Information for

# Synaptic plasticity and handwritten digits recognition of memristor based on high-stability lead-free Cs<sub>3</sub>Bi<sub>2</sub>Br<sub>9</sub> perovskite thin film

Jian Liu,<sup>\*a</sup> Ying Nie,<sup>a</sup> Xiaolong Zhou,<sup>a</sup> Juanjuan Qi,<sup>a</sup> Dongke Li,<sup>b</sup> Jianqiang Luo<sup>c</sup> and Ke Wang<sup>\*ad</sup>

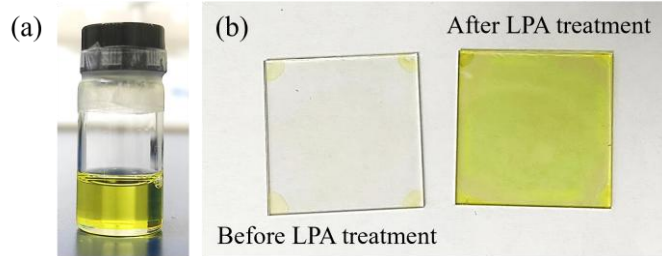
<sup>a</sup> School of Mechanical and Electronic Engineering, East China University of Technology, Nanchang, 330013, China

<sup>b</sup> Hangzhou Global Scientific and Technological Innovation Center, School of Materials Science and Engineering, Zhejiang University, Hangzhou, 311200, China

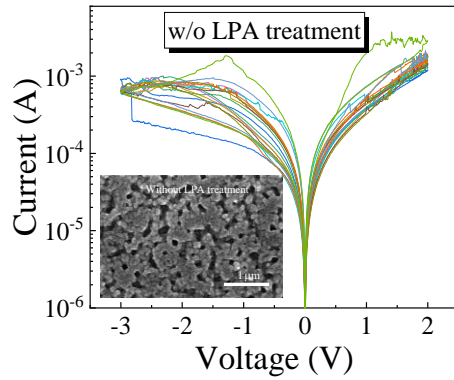
<sup>c</sup> School of Chemistry and Materials Science, East China University of Technology, Nanchang, 330013, China

<sup>d</sup> Jiangxi Province Key Laboratory of Nuclear Physics and Technology, East China University of Technology, Nanchang, 330013, China

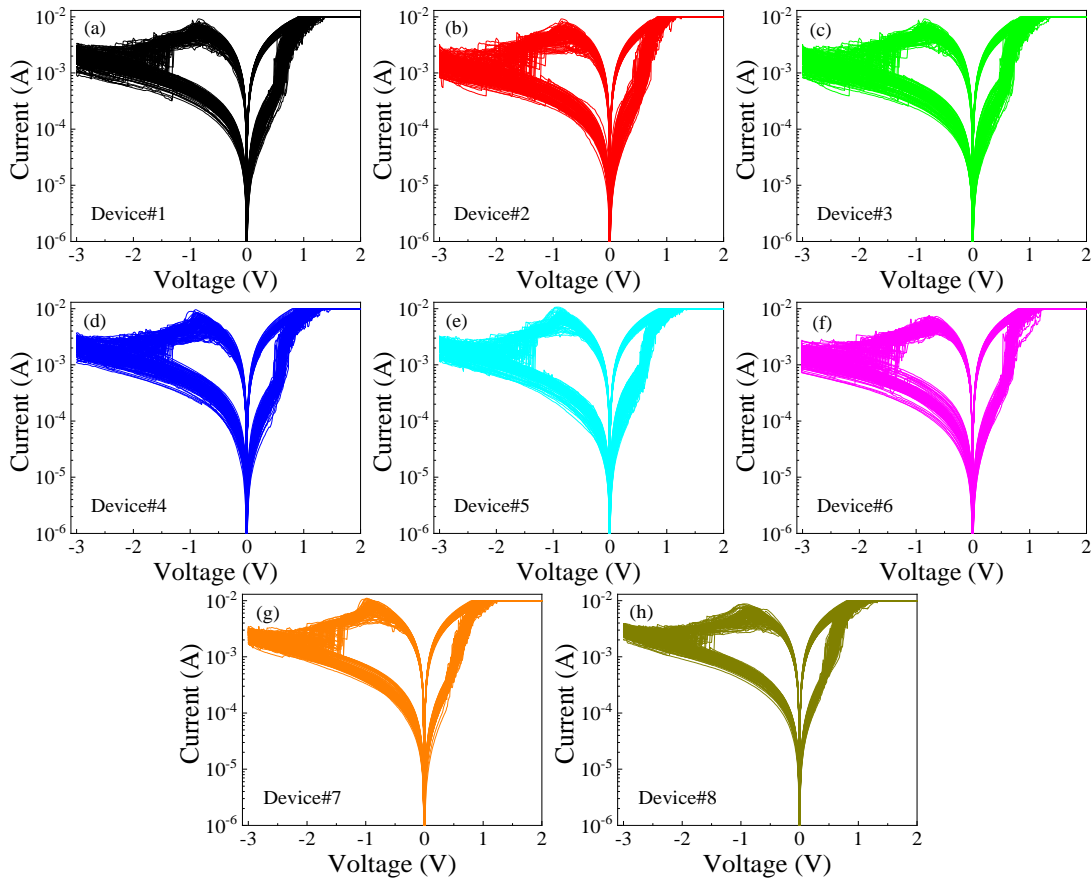
\*Author to whom correspondence should be addressed: [liuj@ecut.edu.cn](mailto:liuj@ecut.edu.cn), [wang@ecut.edu.cn](mailto:wang@ecut.edu.cn)



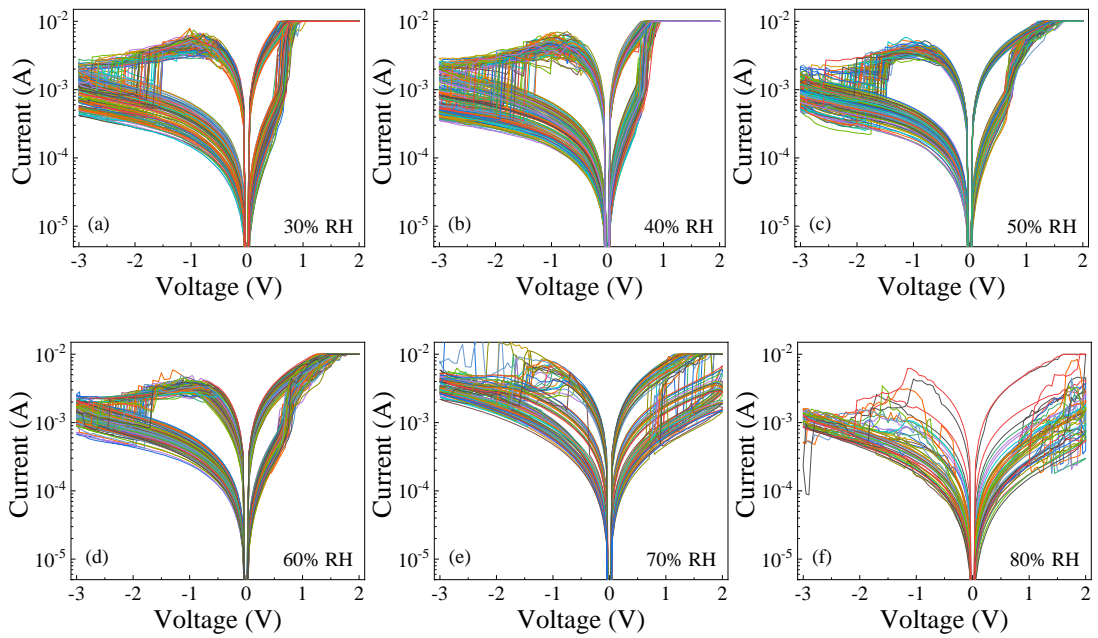
**Fig. S1** Optical micrographs of (a) Cs<sub>3</sub>Bi<sub>2</sub>Br<sub>9</sub> precursor solution and (b) Cs<sub>3</sub>Bi<sub>2</sub>Br<sub>9</sub> film before and after LPA treatment.



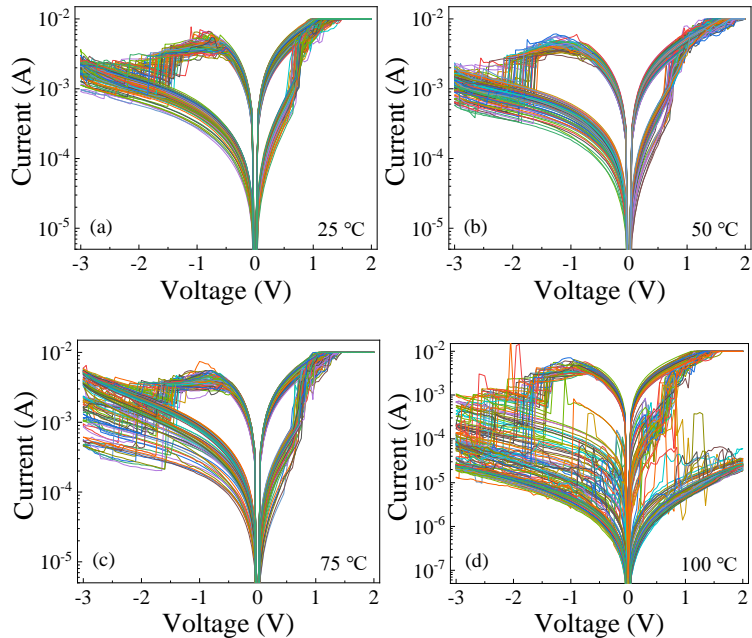
**FIG. S2**  $I$ - $V$  characteristics of the Cs<sub>3</sub>Bi<sub>2</sub>Br<sub>9</sub> thin film memristor without LPA treatment.



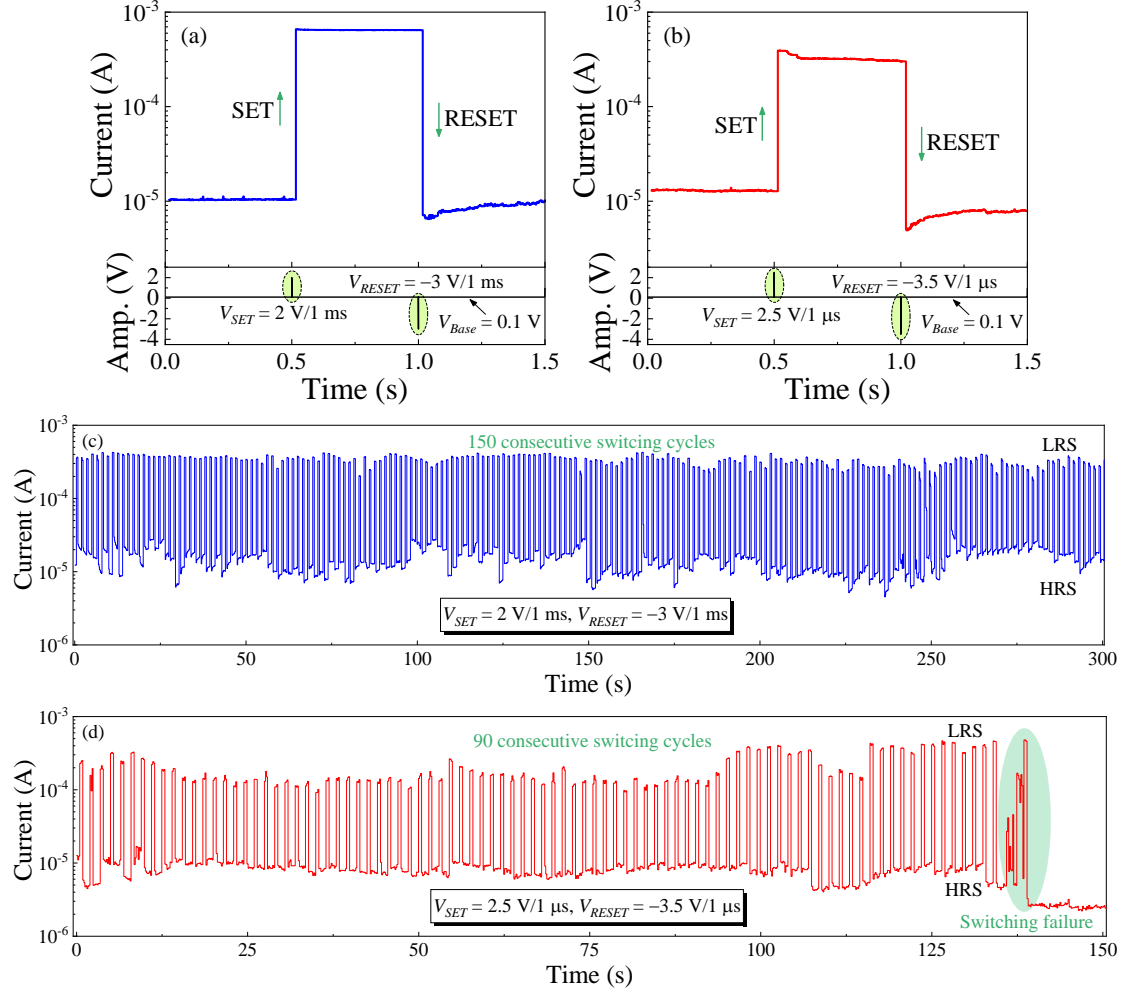
**FIG. S3** Resistive switching performance of 8 devices in different regions of the same sample.



**Fig. S4** Environmental robustness testing of the W/Cs<sub>3</sub>Bi<sub>2</sub>Br<sub>9</sub>/ITO memristor under a relative humidity range of 30% to 80%.



**Fig. S5** Environmental robustness testing of the W/Cs<sub>3</sub>Bi<sub>2</sub>Br<sub>9</sub>/ITO memristor under a working temperature range of 25 to 100 °C.



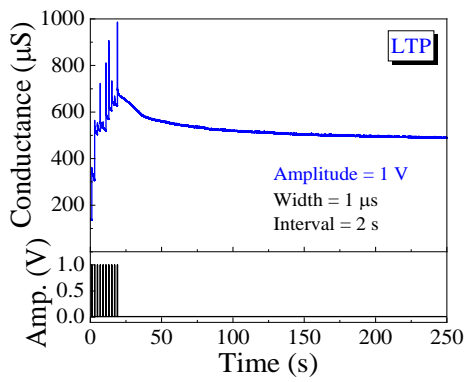
**Fig. S6** Real-time monitoring of SET and RESET switching characteristics: (a) and (b) single pulse switching cycle test with pulse width of ms and  $\mu\text{s}$ , respectively; (c) and (d) consecutive pulse switching cycles test with pulse width of ms and  $\mu\text{s}$ , respectively.

Table S1. Summary of the performance of perovskite-based memristors.

Structure	$R_{HRS}/R_{LRS}$	$V_{SET}$ (V)	$V_{RESET}$ (V)	Endurance	Stability	Reference
Ag/PMMA/CsSnI <sub>3</sub> /Pt	1000	0.13	-0.08	650	/	[1]
Al/Cs <sub>3</sub> Bi <sub>2</sub> I <sub>9</sub> /ITO	10000	0.22	-0.42	410	/	
Al/Cs <sub>3</sub> Bi <sub>2</sub> Br <sub>9</sub> /ITO	10	0.67	-1.21	600	/	[2]
Al/Cs <sub>3</sub> Bi <sub>2</sub> Cl <sub>9</sub> /ITO	100	0.44	-0.97	410	/	
Al/CsBi <sub>3</sub> I <sub>10</sub> /ITO	100	-1.7	0.9	150	2 months	[3]
Au/MAPbI <sub>3-x</sub> Cl <sub>x</sub> /FTO	3	0.8	-0.6	100	/	[4]
Au/Cs <sub>2</sub> AgBiBr <sub>6</sub> /ITO	10	1.53	-3.4	1000	100 days	[5]
Au/(MA) <sub>3</sub> Bi <sub>2</sub> I <sub>9</sub> /ITO	100	1.6	-0.6	300	1 month	[6]
Ag/Cs <sub>3</sub> Cu <sub>2</sub> I <sub>5</sub> /ITO	10	0.6	-0.44	50	/	[7]
Ag/PMMA/Cs <sub>3</sub> Cu <sub>2</sub> I <sub>5</sub> /ITO	100	0.2	-0.45	100	/	
Au/CsPbBr <sub>3</sub> /ITO	10	0.29	-0.22	400	/	[8]
Ag/BA <sub>0.15</sub> MA <sub>0.85</sub> PbI <sub>3</sub> /FTO	1000	-1.1	1.5	1600	/	[9]

Ag/BA <sub>0.15</sub> FA <sub>0.85</sub> PbI <sub>3</sub> /FTO	1000	-0.3	1.2	1000	/	
Au/CsPbBr <sub>3</sub> /Au	10	0.65	-0.98	200	/	[10]
Ag/CsPb <sub>1-x</sub> Bi <sub>x</sub> I <sub>3</sub> /ITO	10	-0.5	3.5	500	5 days	[11]
Ag/Cs <sub>3</sub> Bi <sub>2</sub> I <sub>9</sub> /FTO	1000	0.3	-0.5	1000	1 month	[12]
Ag/Cs <sub>3</sub> Bi <sub>2</sub> Br <sub>9</sub> /ITO	10	-0.5	0.75	3200	7 days	[13]
Al/CsPbBr <sub>3</sub> QD/ITO	100000	-0.45	2.2	1000	200 days	[14]
Al/Cs <sub>2</sub> AgBiBr <sub>5</sub> Cl/ITO	10000	-0.21	1.34	100	100 days	[15]
Ag/(BA) <sub>2</sub> CsAgBi <sub>7</sub> /Pt	10000000	0.13	-0.20	1000	22 days	[16]
W/Cs <sub>3</sub> Bi <sub>2</sub> Br <sub>9</sub> /ITO	10	0.53	-0.83	1100	> 11 months	This work

- [1] Han J S, Le Q V, Choi J, et al. Lead-free all-inorganic cesium tin iodide perovskite for filamentary and interface-type resistive switching toward environment-friendly and temperature-tolerant nonvolatile memories. *ACS applied materials & interfaces*, 2019, 11(8): 8155-8163.
- [2] Luo F, Wu Y, Tong J, et al. Resistive switching and artificial synaptic performances of memristor based on low-dimensional bismuth halide perovskites. *Nano Research*, 2023, 16(7): 10108-10119.
- [3] Xiong Z, Hu W, She Y, et al. Air-stable lead-free perovskite thin film based on CsBi<sub>3</sub>I<sub>10</sub> and its application in resistive switching devices. *ACS applied materials & interfaces*, 2019, 11(33): 30037-30044.
- [4] Yoo E J, Lyu M, Yun J H, et al. Resistive Switching Behavior in Organic-Inorganic Hybrid CH<sub>3</sub>NH<sub>3</sub>PbI<sub>3-x</sub>Cl<sub>x</sub> Perovskite for Resistive Random Access Memory Devices. *Advanced Materials*, 2015, 27(40): 6170-6175.
- [5] Cheng X F, Qian W H, Wang J, et al. Environmentally robust memristor enabled by lead-free double perovskite for high-performance information storage. *Small*, 2019, 15(49): 1905731.
- [6] Hwang B, Lee J S. Lead-free, air-stable hybrid organic–inorganic perovskite resistive switching memory with ultrafast switching and multilevel data storage. *Nanoscale*, 2018, 10(18): 8578-8584.
- [7] Zeng F, Guo Y, Hu W, et al. Opportunity of the lead-free all-inorganic Cs<sub>3</sub>Cu<sub>2</sub>I<sub>5</sub> perovskite film for memristor and neuromorphic computing applications. *ACS applied materials & interfaces*, 2020, 12(20): 23094-23101.
- [8] Luo F, Zhong W M, Tang X G, et al. Application of artificial synapse based on all-inorganic perovskite memristor in neuromorphic computing. *Nano Materials Science*, 2024, 6(1): 68-76.
- [9] Wang Y, Guo D, Jiang J, et al. Element Regulation and Dimensional Engineering Co-Optimization of Perovskite Memristors for Synaptic Plasticity Applications. *ACS Applied Materials & Interfaces*, 2024, 16(10): 12277-12288.
- [10] Liu Z, Cheng P, Kang R, et al. All-Inorganic CsPbBr<sub>3</sub> Perovskite Planar-Type Memristors as Optoelectronic Synapses. *ACS Applied Materials & Interfaces*, 2024, 16(38): 51065-51079.
- [11] Ge S, Wang Y, Xiang Z, et al. Reset voltage-dependent multilevel resistive switching behavior in cspb<sub>1-x</sub>bi<sub>x</sub>i<sub>3</sub> perovskite-based memory device. *ACS applied materials & interfaces*, 2018, 10(29): 24620-24626.
- [12] Li J, Zhang Y, Yao C, et al. Optoelectronic Modulation of Interfacial Defects in Lead-Free Perovskite Films for Resistive Switching. *Advanced Electronic Materials*, 2022, 8(4): 2101094.
- [13] Hu Y, Zhang S, Miao X, et al. Ultrathin Cs<sub>3</sub>Bi<sub>2</sub>I<sub>9</sub> nanosheets as an electronic memory material for flexible memristors. *Advanced Materials Interfaces*, 2017, 4(14): 1700131.
- [14] Cao X, Ma Z, Cheng T, et al. Air-stable, eco-friendly RRAMs based on lead-free Cs<sub>3</sub>Bi<sub>2</sub>Br<sub>9</sub> perovskite quantum dots for high-performance information storage. *Energy & Environmental Materials*, 2023, 6(5): e12419.
- [15] Sun C, Luo F, Ruan L, et al. Enhanced Memristive Performance of Double Perovskite Cs<sub>2</sub>AgBiBr<sub>6-x</sub>Cl<sub>x</sub> Devices by Chloride Doping. *ChemPlusChem*, 2021, 86(11): 1530-1536.
- [16] Kim S Y, Yang J M, Lee S H, et al. A layered (n-C<sub>4</sub>H<sub>9</sub>NH<sub>3</sub>)<sub>2</sub>CsAgBiBr<sub>7</sub> perovskite for bipolar resistive switching memory with a high ON/OFF ratio. *Nanoscale*, 2021, 13(29): 12475-12483.



**FIG. S7** Long-term plasticity (LTP) up to 250 s after pulse-train stimulation is withdrawn.

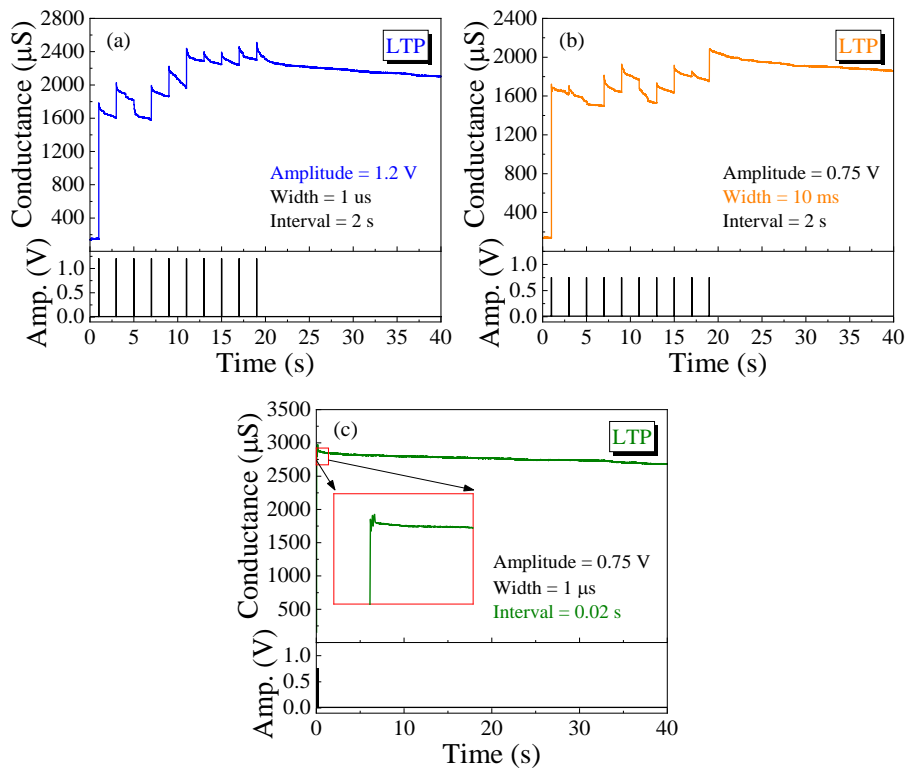


**FIG. S8** Greater amplitude (a) and width (b) of pulse-train or shorter intervals between adjacent pulses (c) result in higher values of the final conductance state when transitioning to LTP.